Inversion-driven free surface multiple modelling using multi-order Green's functions

Gordon Poole and James Cooper, CGG*

Summary

We introduce an inversion-driven free surface multiple modelling scheme based on multi-order Green's functions. The approach optionally combines surface related multiple modelling with source designature and receiver deghosting. We demonstrate the effectiveness of the approach for peg-leg multiple suppression as well as highlighting the benefits of combined receiver deghosting and demultiple. In addition we show how the use of multiples can provide uplift for cable interpolation.

Introduction

Attenuation of shallow water peg-leg multiples remains a challenge for a number of reasons. Although successful in deep water settings, surface-related multiple attenuation (Verschuur et al., 1992) is compromised in shallow water by missing near offsets and insufficient spatial sampling. While τ-p deconvolution is broadly effective, it assumes a locally 1D multiple generator and wavelet truncation is often unavoidable. More recent approaches based on multi-channel prediction operators estimate shallow section multiple generators from multiples (Biersteker, 2001; Hargreaves, 2006; Hung et al., 2010). This reduces the impact of missing near offsets and the poorly recorded water bottom primary reflection. However, the operators can be contaminated by noise and other reflectors.

More recently, Wang et al. (2011) proposed a model-based water-layer demultiple approach based on a known Green's function. For a sufficiently accurate Green's function, the method can predict multiples with a high level of temporal precision. The strategy was extended by Cooper et al. (2015) to improve the amplitude integrity of the model and Huang et al. (2015) to improve the data consistency.

We introduce an inversion-driven free surface multiple modelling technique (MOGIN) using multi-order Green's functions. The approach optionally combines multiple modelling, source designature, receiver deghosting, and cable interpolation.

Methodology

We define a multi-order Green's function (MOGF) as a convolution operator that encodes more than one order of multiple in a single operation. A MOGF may be derived from any single order Green's function representing the Earth response of one or more multiple generators, and includes reflectivity information. In 1D, the multi-order Green's function, M, may be defined as:

$$M = \sum_{i_s=0}^{\infty} G_s^{i_s} \sum_{i_r=0}^{\infty} G_r^{i_r} \qquad (1)$$

where i_s and i_r index multiple orders on source and receiver sides respectively, and G_s, G_r are single order Green's functions representing the multiple generators on source and receiver sides respectively. For consistency, primaries are regarded as multiples of order zero. The magnitude of each summand in (1) is determined by the reflectivity of the multiple generator, which will be less than unity. Each sum is therefore bounded and M is seen to be the product of two binomial expansions as given in equation 2.

$$M = \frac{1}{(1 - G_s)(1 - G_r)} \qquad (2)$$

We define a free surface multiple modelling approach in which the MOGF is used to encode multiples on to an unknown model, such that the known seismic data – comprising primaries and multiples – is recovered in a least squares sense. Working on a frequency slice, the linear equations may be expressed in the form:

$$d = L_g a \qquad (3)$$

where d is the recorded data including multiples, a is the model estimate, and L_g is a convolution operator encoding the MOGF. The resulting model may be used either directly or to drive an estimate of the multiples, which may then be subtracted from the input data. The method may be applied in 1D as above or using higher dimension convolutions on source and receiver sides. In the case 3D convolutions are used, the method may support modelling of 3D multiple generators.

Turning to the case of a locally 1D multiple generator, we extend the resignature inversion equations of Poole et al. (2015) to include 3D receiver re-ghosting and re-multiple using the MOGF operator:

$$d(n) = L(n, m) L_s(m) L_g(m) a(m) \qquad (4)$$

where a is the unknown τ-p domain primary model, L_g is the MOGF convolution operator, L_s is the source resignature operator as described in Poole et al. (2015), and L combines receiver reghost and reverse τ-p slant as described in Wang et al. (2014). The trace index of the common shot domain gather is denoted by n, while m indexes the τ-p domain slowness. Where sampling allows, the equations may be defined in a 5D model space, the τ-p_{sx}-p_{sy}-p_{rx}-p_{ry} domain, where p_{sx} and p_{sy} are the source side slownesses in the *x*- and *y*- directions respectively, p_{rx} and p_{ry} being the corresponding receiver side slownesses. We simplify the approach for towed streamer acquisition by assuming source-receiver ray-path symmetry (as in Poole et al., 2015), thus defining the model in the shot τ-p_{rx}-p_{ry} domain, denoted τ-p_x-p_y for simplicity.

We define the linear operators, beginning with the receiver reghost and reverse slant term:

DOI http://dx.doi.org/10.1190/segam2015-5844229.1

$$L(n,m) = e^{-i\omega\tau_{rxy}(n,m)}\left(e^{i\omega\tau_{rz}(n,m)} + Se^{-i\omega\tau_{rz}(n,m)}\right) \quad (5)$$

$$\tau_{rxy}(n,m) = o_x(n)p_x(m) + o_y(n)p_y(m) \quad (6)$$

$$\tau_{rz}(n,m) = r_z(n)p_z(m) \quad (7)$$

where o_x and o_y are source-receiver offsets in the *x*- and *y*-directions, r_z is the receiver depth, and p_x, p_y, and p_z are *x*-, *y*-, and *z*-direction slownesses. The first exponential term in (5) relates to the reverse slant operator. The subsequent bracketed exponential terms relate to receiver ghost encoding, S being the free surface reflectivity which can, for example, be taken to be equal to -1. The slownesses in each direction are related to the water velocity, v_w, by the following expression:

$$\frac{1}{v_w^2} = p_x^2(m) + p_y^2(m) + p_z^2(m) \quad (8)$$

Next, the source side directional resignature term may be expanded as:

$$L_s(m) = \sum_{h=1}^{H}\left[N(h)e^{-i\omega\tau_{sxy}(h,m)}\left(e^{i\omega\tau_{sz}(h,m)} + Se^{-i\omega\tau_{sz}(h,m)}\right)\right] \quad (9)$$

$$\tau_{sxy}(h,m) = g_x(h)p_x(m) + g_y(h)p_y(m) \quad (10)$$

$$\tau_{sz}(h,m) = g_z(h)p_z(m) \quad (11)$$

The directional resignature operators defining L_s are calculated by beam forming H notional sources, $N(h)$, which describe the source emission as per Ziolkowski et al. (1982). g_x and g_y relate to the notional source positions relative to the center of the source in the *x*- and *y*-directions, respectively. g_z is the notional source depth relative to the sea surface. The bracketed exponential terms define the reghosting operator of the notional sources.

Assuming a locally 1D multiple generator, for example relating to the water bottom, the slowness-dependent MOGF operator, L_g, may be defined with reference to (2) in terms of single order Green's functions, viz.

$$L_g = \frac{1}{(1 - R_s e^{-2i\omega z_s p_z})(1 - R_r e^{-2i\omega z_r p_z})} \quad (12)$$

where R_s and z_s are, respectively, the source side water bottom reflectivity and depth, with R_r and z_r the corresponding quantities for the receiver side. In this way, we allow both the reflectivity and the depth of the water bottom to be spatially variant. Ideally, the amplitude of the Green's function should vary with reflection angle and incorporate spherical spreading, although inaccuracies in this regard may be compensated for, at least partially, through use of mild adaptive subtraction.

Equation 4 may be formulated in the time or frequency domain and solved with iteratively re-weighted least squares inversion (Trad et al., 2003) using any combination of the linear operators. The receiver deghosting and demultiple may be implemented separately with independent inversions. Alternatively, the corresponding operators may be used in a joint inversion to achieve simultaneous deghosting and demultiple. The advantage of the latter approach is that the modelled multiples can be used to constrain the modelling of the receiver ghost.

Once the model has been found, it may be used to output the primary estimate directly. Alternatively, it may be used to output energy to subtract from the input, for example multiples in the case of demultiple, or receiver ghost energy in the case of receiver deghosting. By modifying the MOGF term, it is possible to output individual multiple orders suitable for use in a multi-model adaptive subtraction (Mei and Zou, 2010).

The strategy may also be used for cable interpolation, redatum, or extrapolation, in which case the coordinates relating to the equations are modified for a final application of the linear operators to generate data at the required output positions. The multiple reflections encoded by the MOGF can be used to improve the spatial sampling of the input data and assist the cable interpolation. The equations may also be modified to work with multi-sensor data, for example following Poole (2014).

Synthetic data example

The synthetic data examples were based on an acquistion using 12 variable depth streamers (8 m to 50 m depth) with 100 m separation, an inline near offset of 100 m, and 480 channels per cable at 12.5 m spacing. The data was generated using Kirchhoff modelling with a 1D Earth model from the North Sea. The water depth was 100 m.

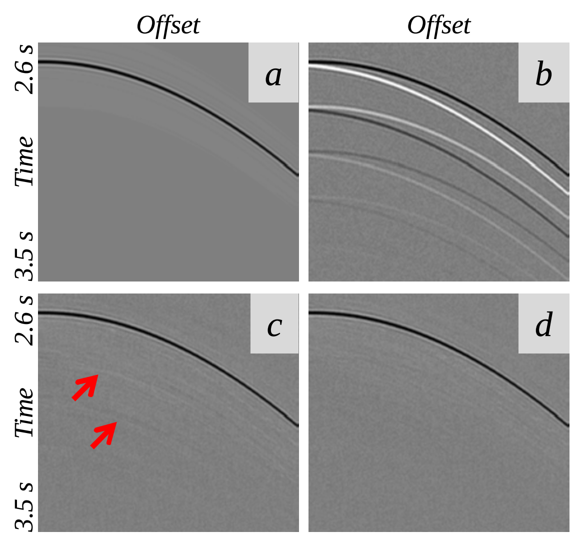

Figure 1: Synthetic data for: (a) primary reflection; (b) primary with water-layer peg-leg multiples, receiver ghost and Gaussian noise; (c) after sequential receiver deghosting and demultiple; (d) combined receiver deghosting and demultiple.

DOI http://dx.doi.org/10.1190/segam2015-5844229.1

The first synthetic example was based on a horizontal primary reflector at 3.2 km depth and peg-leg water layer multiples. Figure 1a shows reference primary data for an outer cable. Figure 1b shows the input data used for the MOGIN algorithm, comprising primary, multiples, receiver ghosts and Gaussian noise. Figure 1c shows the data after sequential applications of receiver deghosting and peg-leg demultiple using the proposed approach. Figure 1d shows the data after simultaneous receiver deghosting and peg-leg demultiple using the proposed approach. The results show a small reduction in residual multiple in the case receiver deghosting and demultiple are applied simultaneously.

The second synthetic example was based on an out-of-plane primary diffraction at 3.2 km depth and 3 km to the side of the spread The modelled data consisted of the primary, together with receiver ghost and receiver side peg-leg multiples (using a local 1D assumption for the generators) and Gaussian noise. These data are shown in Figure 2a, for part of a common shot gather on an inner cable. The primary and multiples are annotated in the figure by M_i^U, where i is the order of the multiple. The corresponding receiver ghost events are annotated by M_i^D. Figure 2c shows the same modelled data but for a single near channel and across all 12 cables, highlighting the strong out-of-plane character of the modelled events.

Simultaneous receiver deghosting and peg-leg demultiple was applied to the data. Results after MOGIN are shown in Figures 2b and 2d, corresponding respectively to the input shown in Figures 2a and 2c. These displays illustrate the effectiveness of the method at handling peg-leg multiples relating to a locally 1D reflector where the primary is outside the cable spread.

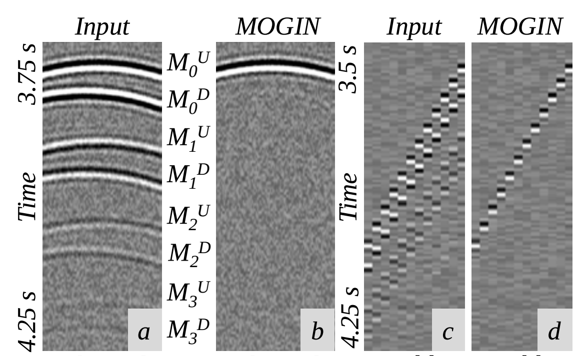

Figure 2: Combined receiver deghosting and peg-leg demultiple. (a) shot gather, input; (b) shot gather, 3D joint receiver deghost and peg-leg demultiple; (c) cross-cable, input; (d) cross-cable, 3D joint receiver deghost and peg-leg demultiple.

Real data example

The real data example comes from variable depth streamer acquisition in the North Sea. The acquisition deployed dual-level airgun source arrays (Siliqi et al., 2013) and towed 10 streamers with 100 m separation. Pre-processing included swell noise attenuation and source designature.

An example of cable interpolation is given in Figure 3, in which each group of traces comprises a single channel across all cables. Figure 3a shows the 10 acquired cables with 100 m separation. Figures 3b and 3c show results of cable interpolation to 12.5 m separation using, respectively, a standard τ-p sparse model, and a τ-p model derived using the MOGF term. The interpolation result using the MOGF term shows improved spatial consistency and less aliasing-related noise. This is because interpolation using the MOGF term exploits the improved sampling relating to the multiple reflections at the sea surface.

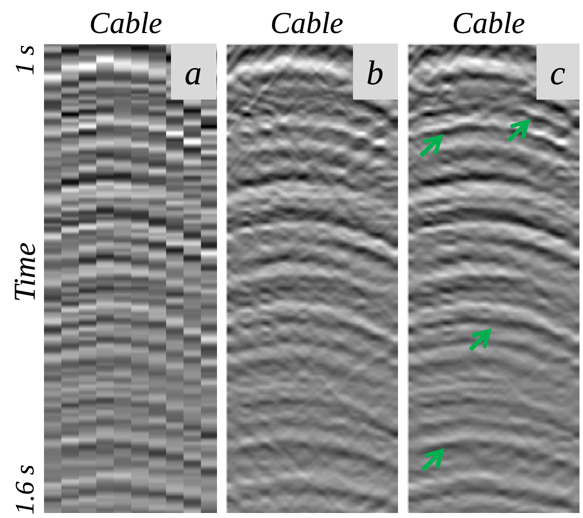

Figure 3: Cable interpolation comparison. (a) input data; (b) cable interpolation using a standard sparse τ-p model; (c) cable interpolation using the MOGF term in the MOGIN algorithm.

As with the synthetic example (Figure 1), we compared receiver deghosting followed by peg-leg demultiple, with simultaneous receiver deghosting and peg-leg demultiple. The results, shown in Figure 4, demonstrate an improvement in coherency of the low frequencies when using the simultaneous approach.

Finally the MOGIN algorithm was used to compare simultaneous receiver deghosting and demultiple in 2D and 3D. Results are presented for 2D inline stacks of an inner cable. Figure 5a shows data prior to receiver deghosting and demultiple. Figure 5b shows the result of using MOGIN for deghosting only. Figure 5c shows 2D simultaneous deghosting and demultiple, in which only the inner cable has been used in the MOGIN algorithm. Figure 5d shows 3D application of MOGIN for simultaneous deghosting and demultiple, in which all cables have been used in the algorithm. The observed differences between the 2D and 3D results are small across those areas of the section where the geology is least complex; however, the

DOI http://dx.doi.org/10.1190/segam2015-5844229.1

boxes annotated on the figure highlight the significant benefits of the 3D approach in the presence of strong out-of-plane diffractors.

Conclusions

We have introduced a flexible, inversion-based surface related multiple modeling algorithm using multi-order Green's functions (MOGIN). The algorithm optionally combines the operations of source designature, receiver deghosting, demultiple, and interpolation into a single scheme. The strategy benefits from the increased spatial sampling in the multiples based on the sea surface reflections. We propose an efficient method assuming source-receiver ray-path symmetry and a locally 1D multiple generator. The effectiveness of this method has been demonstrated for joint receiver deghosting and attenuation of out of plane multiples on a real North Sea data example. The use of multiple modelling has also been shown to benefit cable interpolation.

Acknowledgements

We thank CGG Multi-Client for the Cornerstone data examples and CGG for permission to publish this work. Thanks to Peng Zhao and Vetle Vinje for assistance with generating the synthetic examples.

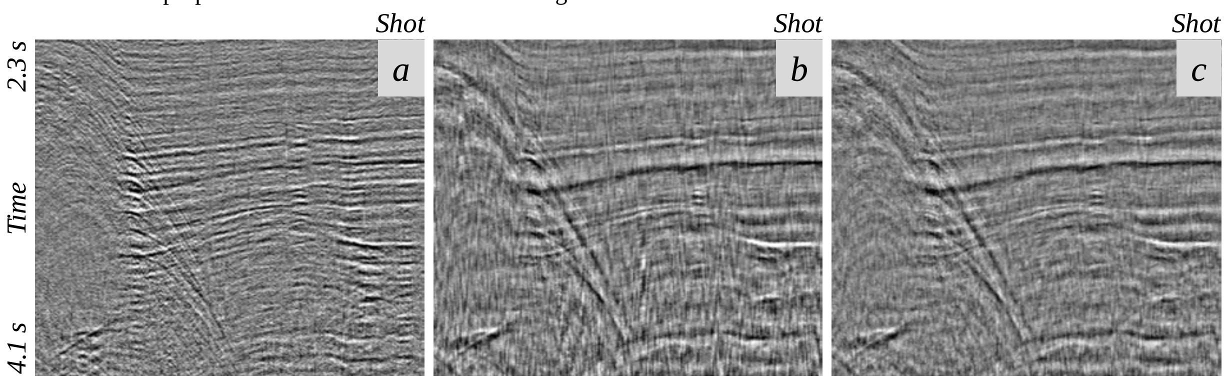

Figure 4: Near channel display comparing: (a) input including multiples and receiver ghosts; (b) receiver deghosting followed by peg-leg demultiple; (c) simultaneous receiver deghosting and peg-leg demultiple.

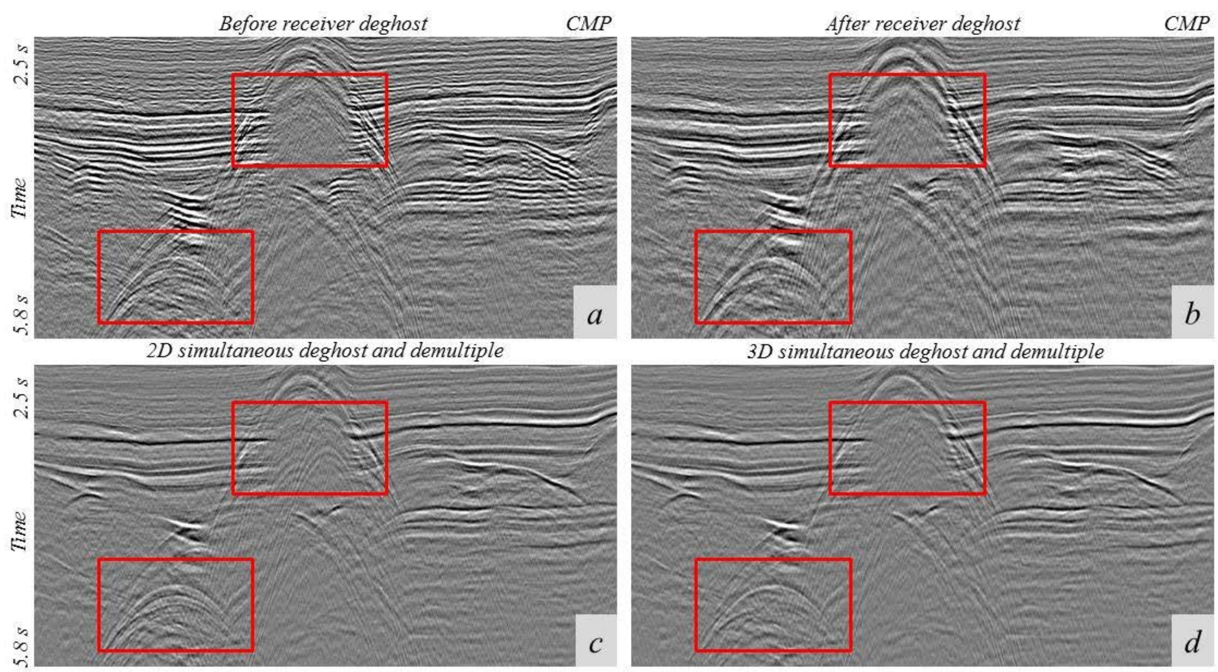

Figure 5: 2D inline stacks for an inner streamer: (a) before receiver deghost; (b) after 3D receiver deghost with MOGIN; (c) after 2D simultaneous receiver deghost and demultiple with MOGIN; (d) after 3D simultaneous receiver deghost and demultiple with MOGIN.

EDITED REFERENCES

Note: This reference list is a copyedited version of the reference list submitted by the author. Reference lists for the 2015 SEG Technical Program Expanded Abstracts have been copyedited so that references provided with the online metadata for each paper will achieve a high degree of linking to cited sources that appear on the Web.

REFERENCES

Biersteker, J., 2001, MAGIC: Shell's surface multiple attenuation technique: 71st Annual International Meeting, SEG, Expanded Abstracts, 1301–1304.

Cooper, J., G. Poole, R. Wombell, and P. Wang, 2015, Recursive model-based water-layer demultiple: Presented at the 77th Annual International Conference and Exhibition.

Hargreaves, N., 2006, Surface multiple attenuation in shallow water and the construction of primaries from multiples: 76th Annual International Meeting, SEG, Expanded Abstracts, 2689–2693.

Huang, H., P. Wang, and S. Hu, 2015, Selective-input adaptation of model-based water-layer demultiple: Presented at the 77th Annual International Conference and Exhibition, EAGE.

Hung, B., L. Yang, J. Zhou, and Q. L. Xia, 2010, Shallow water demultiple: 21st Geophysical Conference, ASEG, Extended Abstracts, 1–4.

Mei, Y., and Z. Zou, 2010, A weighted adaptive subtraction for two or more multiple models: 80th Annual International Meeting, SEG, Expanded Abstracts, 3488–3492.

Poole, G., 2014, Wavefield separation using hydrophone and particle velocity components with arbitrary orientation: 84th Annual International Meeting, SEG, Expanded Abstracts, 1858–1862, doi: 10.1190/segam2014-0756.1.

Poole, G., J. Cooper, S. King, and P. Wang, 2015, 3D source designature using source-receiver symmetry in the shot tau-px-py domain: Presented at the 77th Annual International Conference and Exhibition, EAGE.

Siliqi, R., T. Payen, R. Sablon, and K. Desrues, 2013, Synchronized multilevel source, a robust broadband marine solution: 83rd Annual International Meeting, SEG, Expanded Abstracts, 56–60.

Trad, D., T. Ulrych, and M. Sacchi, 2003, Latest views of the sparse Radon transform: Geophysics, **68**, 386–399. http://dx.doi.org/10.1190/1.1543224.

Verschuur, D. J., A. J. Berkhout, and C. P. A. Wapenaar, 1992, Adaptive surface-related multiple elimination: Geophysics, **57**, 1166–1177. http://dx.doi.org/10.1190/1.1443330.

Wang, P., H. Jin, S. Xu, and Y. Zhang, 2011, Model-based water-layer demultiple: 81st Annual International Meeting, SEG, Expanded Abstracts, 3551–3555.

Wang, P., S. Ray, and K. Nimsaila, 2014, 3D joint deghosting and crossline interpolation for marine single-component streamer data: 84th Annual International Meeting, SEG, Expanded Abstracts, 3594–3598.

Ziolkowski, A., G. E. Parkes, L. Hatton, and T. Haughland, 1982, The signature of an air-gun array: computation from near-field measurements including interactions: Geophysics, **47**, 1413–1421. http://dx.doi.org/10.1190/1.1441289.

DOI http://dx.doi.org/10.1190/segam2015-5844229.1